

# Nanoscale, Phonon-Coupled Calorimetry with Sub-Attojoule/Kelvin Resolution

W. Chung Fon,<sup>†</sup> Keith. C. Schwab,<sup>‡</sup> John M. Worlock,<sup>†,§</sup> and Michael L. Roukes<sup>\*,†</sup>

Condensed Matter Physics, California Institute of Technology 114-36, Pasadena, California 91125, and Laboratory for Physical Sciences, University of Maryland, College Park, Maryland 20740, and Department of Physics, University of Utah, Salt Lake City, Utah 84112

Received July 14, 2005; Revised Manuscript Received August 5, 2005

## ABSTRACT

We have developed an ultrasensitive nanoscale calorimeter that enables heat capacity measurements upon minute, externally affixed (phonon-coupled) samples at low temperatures. For a 5 s measurement at 2 K, we demonstrate an unprecedented resolution of  $\Delta C \sim 0.5$  aJ/K ( $\sim 36$  000  $k_B$ ). This sensitivity is sufficient to enable heat capacity measurements upon zeptomole-scale samples or upon adsorbates with sub-monolayer coverage across the minute cross sections of these devices. We describe the fabrication and operation of these devices and demonstrate their sensitivity by measuring an adsorbed  $^4\text{He}$  film with optimum resolution of  $\sim 3 \times 10^{-5}$  monolayers upon an active surface area of only  $\sim 1.2 \times 10^{-9}$  m<sup>2</sup>.

Calorimetry is a powerful technique that is widely employed to measure the enthalpy of chemical reactions<sup>1</sup> and the heat capacity<sup>2</sup> and other physical properties of solid-state systems. Currently, microcalorimeters produced by semiconductor processing techniques are routinely used for measurement of the heat capacity of thin films and the heat of reaction for processes such as catalytic dissociation of carbon monoxide molecules on nickel.<sup>3</sup> Current state-of-the-art microcalorimeters have a resolution that is typically of order  $\sim 1$  fJ/K, limited by the addendum (the heat capacity of the calorimeter itself) and the sensitivity of thermometry employed.<sup>3,4</sup> The quest to improve this sensitivity is not simply to improve the accuracy of measurement but, more importantly, to enable heat capacity measurement of nanoscale objects and samples such as very thin films (e.g., epitaxial layers of magnetic semiconductors), fullerenes, nanoparticles and nanoclusters, biological macromolecules, and the heat of reaction of individual molecules. In this paper, we demonstrate a suspended silicon nitride (SiN) calorimeter integrated with AuGe resistance thermometry. The device exhibits an optimum resolution of  $\sim 0.5$  aJ/K at 2 K. We discuss the fabrication, operation, and resolution of such devices and demonstrate their use by measuring the low-temperature heat capacity of an adsorbed helium gas film at sub-monolayer coverage over the device area  $A \sim 1.2 \times 10^{-9}$  m<sup>2</sup> (1200  $\mu\text{m}^2$ ).

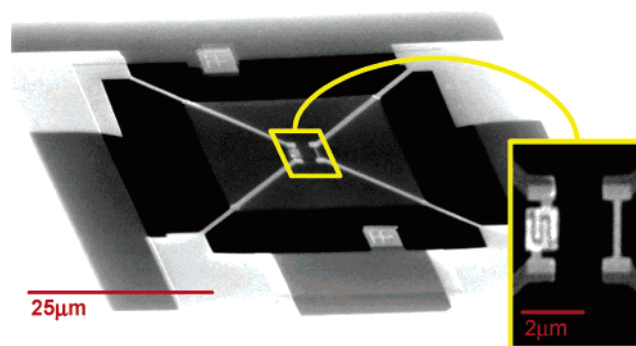


**Figure 1.** Electron micrograph of the suspended calorimeter. The inset shows a magnified view of the central portion of the suspended region, displaying the interdigitated thermometer (left) and Au heater (right).

In Figure 1 we show a scanning electron micrograph of the calorimeter. The suspended body of the calorimeter is a  $25 \times 25 \mu\text{m}^2$  “plate” patterned from a 120 nm thick SiN membrane. Four  $8 \mu\text{m}$  long and 600 nm wide SiN beams suspend the calorimeter body from the substrate and provide its thermal contact to the environment. At the center of the calorimeter body, there are two nanofabricated transducers: a Au heater and a AuGe thermometer for in situ heating and temperature measurement. Thin film Nb leads running on top of the beams connect the heater and thermometer to the substrate. These provide electrical contact to the transducers, without adding parasitic thermal contact to the environment for temperatures below  $T_c(\text{Nb}) \approx 8$  K where electronic thermal transport becomes an important pathway.

\* Correspondence and request for materials should be addressed to M.L.R. (e-mail: roukes@caltech.edu).

<sup>†</sup> California Institute of Technology.

<sup>‡</sup> University of Maryland.

<sup>§</sup> University of Utah.

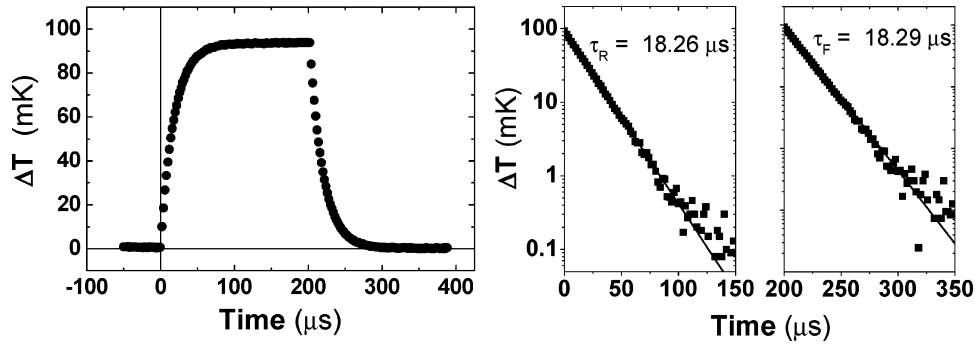


**Figure 2.** The time domain response of calorimeter temperature at  $T = 4.5$  K in response to a heat pulse. The heat pulse power while on is  $0.125$  nW, the rise in temperature is  $\Delta T = 93.4$  mK, and the rising and falling time constants are  $\tau_R = 18.26 \pm 0.002 \mu\text{s}$  and  $\tau_F = 18.29 \pm 0.002 \mu\text{s}$ , respectively. From these traces, which represent the average of  $2 \times 10^5$  separate measurements, we deduce the thermal conductance,  $G = 1.34$  nW/K, and the heat capacity,  $C = 24.5$  fJ/K. The discrepancy between the rising and falling time constants does not come from the experimental measurement error. Instead, it is due to the variation of thermal relaxation time at the different temperature (the rising pulse is at  $4.5$  K while the falling pulse is at  $4.5 + 0.0934 = 4.5934$  K). To better approximate the heat capacity at a particular temperature, we adopt the rising pulses for heat capacity measurement.

The device is fabricated by electron beam lithography, electron cyclotron resonance (ECR) plasma etching, and metal film deposition. The SiN membrane is patterned, using a standard backside KOH etch, from a low-stress SiN film deposited by low-pressure chemical vapor deposition on a silicon substrate. The AuGe thermometer is deposited by sequential elemental layer deposition.<sup>5</sup> To tailor the thermometer for high-speed measurement, the AuGe material is deposited between two interdigitated gold electrodes; this limits the two-terminal transducer resistance by minimizing its effective path length. The proximity of these Au electrodes also serves to enhance thermalization between electrons and phonons in the sensor, thereby minimizing electron heating effects.<sup>6</sup> Superconducting electrical leads provide connection to wirebond pads; these are formed by subtractive patterning of plasma-deposited Nb. At  $2$  K, the measured resistances of the heater and thermometer are  $\sim 22 \Omega$  and  $\sim 12$  k $\Omega$ , respectively.

The small total volume of metallic heater and thermometer elements ensures a minuscule contribution of heat capacity to the addendum (i.e., the calorimeter itself). This is particularly important below  $0.5$  K where the electronic heat capacity of the transducers become dominant. High-speed thermometry ( $\geq 200$  kHz bandwidth) is necessary to track the fast relaxation of the calorimeter (relaxation time  $\tau \sim 20$  to  $100 \mu\text{s}$ ). In this regard, previous realizations of sensitive thermometers based upon superconducting tunnel junctions and Mott insulators ( $Z > 1$  M $\Omega$ ) are undesirable since their high impedance necessitates complex readout schemes to yield high bandwidths.<sup>7</sup> Our AuGe thin film thermometers provide temperature coefficients,  $(1/R_{\text{th}})(\partial R_{\text{th}}/\partial T)$ , of about  $0.01/\text{K}$ , with two-terminal impedance below  $20$  k $\Omega$ . For these thermometers, the sensing current is limited by electron-phonon decoupling<sup>6</sup> to  $\leq 20$  nA for  $T < 0.5$  K. This maximum applicable sensing current determines the sensitivity of the thermometer and ultimately limits its usefulness at the lowest temperatures.

We characterize the calorimeter and demonstrate its operation by measuring its addendum heat capacity in the time domain. First, the device is cooled in a  $^3\text{He}$  cryostat

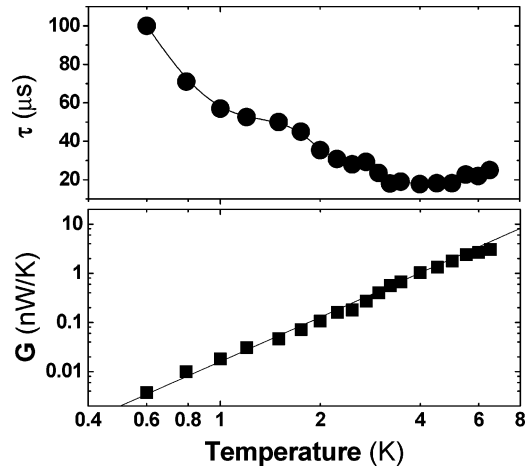
**Table 1.** Heat Capacity Contribution from the Various Components of the Calorimeter

| calorimeter component   | $C(T = 0.6 \text{ K})$ | $C(T = 2 \text{ K})$    | $C(T = 6 \text{ K})$ |
|-------------------------|------------------------|-------------------------|----------------------|
| device total (measured) | 0.38 fJ/K              | 3.75 fJ/K               | 58 fJ/K              |
| SiN Debye (calculated)  | 0.01 fJ/K              | 0.43 fJ/K               | 12 fJ/K              |
| Au heater and           | 2.4 aJ/K               | 9 aJ/K                  | 27 aJ/K              |
| AuGe thermometer        | 1.6 aJ/K               | 6 aJ/K                  | 18 aJ/K              |
| Nb leads (electronics)  | negligible             | $3 \times 10^{-23}$ J/K | 6 aJ/K               |

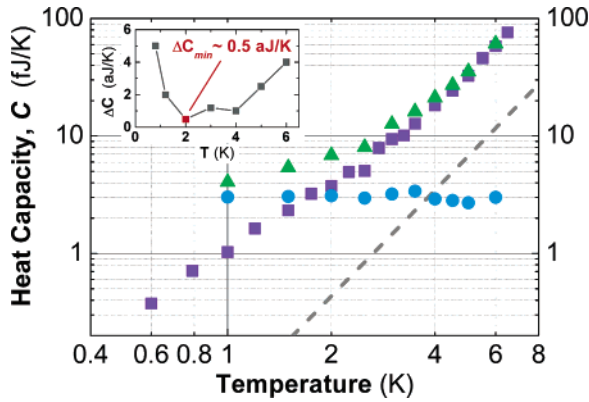
and the AuGe thermometer is calibrated against a commercial NTD Ge thermometer. The temporal evolution of the voltage drop across the thermometer is amplified by a low noise preamplifier and subsequently captured by a fast digital oscilloscope. To measure the heat capacity, a current pulse, of power  $P$ , is applied to the heater. In response to this stimulus, the temperature of the calorimeter rises as  $T = T_0 + (P/G)(1 - e^{-t/\tau})$ . Here,  $G$  is the thermal conductance,  $\tau$  is the thermal relaxation time constant of the calorimeter, and  $t = 0$  denotes the rising edge of the heat pulse. From the time domain response that is captured, we extract  $G$  and  $\tau$ , which yields the heat capacity through the relation  $C = G\tau$ . To improve accuracy, the measurement is repeated and averaged  $\sim 10^6$  times, requiring a total sampling interval of less than  $5$  s.

Figure 2a shows measurements of the exponential response of the calorimeter's temperature due to the heat pulses at  $T = 4.5$  K. From this response, we determine the addendum heat capacity to be  $C = 24.5$  fJ/K. The measured thermal conductance and thermal relaxation time constant for  $0.6 \text{ K} < T < 8 \text{ K}$  are displayed in Figure 2b. The resultant addendum heat capacity is plotted as a function of  $T$  in Figure 2c.

In the temperature regime of these studies, the heat capacity of the calorimeter is always dominated by that of the SiN calorimeter body. Contributions from the phonon and electron heat capacity of the heater, thermometer, and leads are, by comparison, relatively small. Our estimates for these are displayed in Table 1. In Figure 4 we also show that the measured addendum heat capacity is significantly larger than the Debye phonon heat capacity of the calorimeter body itself (estimated to be  $\sim 0.05$  fJ/K).<sup>8</sup> Previous studies



**Figure 3.** The thermal relaxation time,  $\tau$ , and the thermal conductance,  $G$ , of the calorimeter measured from 0.6 to 7 K. The latter follows expectations for diffusive phonon transport involving a boundary-scattering-limited mean free path; the displayed fit yields  $G = 0.016T^3$  (nW/K).



**Figure 4.** The heat capacity of the calorimeter (violet), the heat capacity of calorimeter with adsorbed He gas film (green), and the heat capacity of the He gas film (blue). The He gas coverage is  $\sim 0.16$  monolayer over the device. The dashed gray line represents the estimated Debye phonon heat capacity of the calorimeter. Inset: Measurement resolution attained at various temperatures by the calorimeter for 5 s averaging time. Highest resolution,  $\Delta C \sim 0.5$  aJ/K ( $\sim 36000k_B$ ), is attained at 2 K in these experiments.

lead us to believe this extra heat capacity may originate from defects, i.e. from the tunneling motional states of the ions within the amorphous SiN layers.<sup>9</sup> To estimate the contribution of the tunneling states to heat capacity, we model them as two-level systems with a white spectrum of activation energies between 0 and 100 K.<sup>10</sup> From this we deduce that a density of  $10^{18}$  cm<sup>-3</sup> of tunneling states would be sufficient to account for the excess heat capacity. This is similar in magnitude to what is observed in vitreous silica.<sup>8</sup> The phonon mean free path is deduced from the thermal conductance using a simple diffusive transport picture; it is found to be  $\lambda_{ph} \approx 0.2$   $\mu\text{m}$ .<sup>11</sup> This short mean free path is consistent with previous measurements upon nanoscale devices<sup>10,12</sup> and appears to arise from the strong surface scattering of phonons.

We evaluate the observed *resolution* of heat capacity for these nanoscale calorimeters,  $\Delta C$ , by computing the uncertainty in the addendum measurement. One thousand time-synchronized measurements of the pulse-heating response

are averaged to provide mean exponential rise and decay times. From these we obtain an average value for the addendum heat capacity. This process is repeated one hundred times to obtain to measure the statistical variations of this heat capacity. We assume the distribution of measured values is Gaussian and employ a nonlinear least-squares fit to extract the mean value of the heat capacity and its variance. The square root of the latter represents the measurement resolution,  $\Delta C$ , attained with our devices. As seen in the inset of Figure 4, the heat capacity resolution is less than 2 aJ/K over a temperature range from  $\sim 1$  to 5 K, with a minimum of 0.5 aJ/K attained at 2 K.

The high resolution of the calorimeter is attained primarily because of the very small addendum of the device. This, in turn, is largely a consequence of the small volume of the SiN calorimeter body. Below 2 K, nonetheless, it becomes important to control the electronic heat capacity in the heater, thermometer, and leads to maintain a small relative contribution from these components. For this reason, as mentioned, we employ nanoscale transducers to obtain very small transducer volumes and employ superconducting electrical connections to these transducers to preclude parasitic thermal coupling through such connections to the calorimeter body.

The theoretical resolution of the calorimeter can be written as

$$\Delta C(T) = \frac{1}{\Delta V_{th}(T)} \left[ \frac{2S_V(T)\Delta f}{N} \right]^{1/2} C(T) = \frac{1}{PI_{th}[\partial R(T)/\partial T]} \left[ \frac{S_V(T)G(T)^3 C(T)}{2\pi N} \right]^{1/2} \quad (1)$$

where  $S_V$  is the effective spectral density of the voltage noise (from all sources, referred to the transducer's output),  $\Delta V_{th} = (P/G)(\partial R/\partial T)I_{th}$  the (asymptotic) root mean square (rms) voltage signal from the thermometer in response to continuous application of heater power  $P$ ,  $\Delta f \sim G/(2\pi C)$  the maximum single-shot measurement bandwidth,  $N$  the number of repeated measurements, and  $I_{th}$  the thermometer sensing current. In eq 1 we have denoted terms that are explicitly temperature dependent. However, it should be noted that implicit limitations to  $P$  and  $I_{th}$  arise from these explicit dependencies. The principal contributions to  $S_V$  arise from the transducers  $1/f$  noise and readout amplifier noise. In these experiments the  $1/f$  noise is predominant, and yields  $\sqrt{(S_V\Delta f)} \sim 10$  nV for  $\Delta f \sim 1$  MHz. For  $T \sim 2$  K, using eq 1 and values from Table 1 yields a predicted resolution of  $\Delta C \sim 0.34$  aJ/K for a measurement integration time of  $t \sim 20$  s (i.e.,  $N = t/\tau \sim 100k$ ). Optimal resolution is attained at 2 K: above this temperature resolution decreases with the increasing addendum of the calorimeter; below this the calorimeter resolution is degraded by electron heating (which restricts usable thermometer sensing current and thereby compromising its sensitivity).

To demonstrate operation of the calorimeter, we have measured the low-temperature heat capacity of an adsorbed <sup>4</sup>He film at sub-monolayer coverage over the very small active surface area of the calorimeter,  $\sim 1.2 \times 10^{-9}$  m<sup>2</sup>. A

coverage of  $\approx 2$  atoms/nm<sup>2</sup> ( $\sim 0.16$  monolayers) was accreted upon the cooled calorimeter by exposing it to a carefully controlled pressure of helium gas. The heat capacity of the film was measured to be  $\approx 3$  fJ/K (Figure 4), which corresponds to a heat capacity of  $1.4 k_B$  per helium atom. This value is similar to that observed for He adsorbed on Grafoil, where the adsorbed gas apparently behaves like a two-dimensional ideal gas.<sup>13</sup>

Further development of the calorimeter can improve its sensitivity and operating range. Reduction of the device to yet smaller size, and utilization of material with smaller heat capacity for the calorimeter body (e.g., SiC) would serve to improve the sensitivity by 1 to 2 orders of magnitude. For operation below 0.3 K, more exotic thermometry, such as SQUID-based noise thermometry<sup>14</sup> and superconducting tunneling junctions read out by an RF-SET,<sup>15</sup> could be applied. The calorimeter could also be converted into a bolometer with possible advantages of high sensitivity and high operation temperature (1.2–4 K), although small device cross section must be considered. Replacement of the Nb leads with leads patterned from a thin film of normal metal (e.g., Au) should permit applications from 5 K to room temperature. This should only minimally degrade the calorimeter's overall performance in this regime, since the electronic heat capacity and thermal conduction of normal metal leads become quite small above 5 K. Moreover, the strong electron phonon coupling at these temperatures should ensure heat generated in the heater is efficiently transferred to the lattice.

We have developed an ultrasensitive calorimeter, suitable for phonon-coupled heat capacity measurements, that pro-

vides unprecedented resolution of  $\sim 0.5$  aJ/K measured at 2 K. We anticipate that this type of calorimetric device should find important applications in heat capacity measurement upon a wide variety of nanometer-scale samples.

**Acknowledgment.** We gratefully acknowledge support for this work from the NSF through Grant DMR-0102886.

## References

- (1) Todd, M. J.; Gornez, J. *Anal. Biochem.* **2001**, *296*, 179.
- (2) Denlinger, D. W.; Abarra, E. N.; Allen, K.; Rooney, P. W.; Messer, M. T.; Watson, S. K.; Hellman, F. *Rev. Sci. Instrum.* **1994**, *65* (4), 946.
- (3) Borroni-Bird, C. E.; King, D. A. *Rev. Sci. Instrum.* **1991**, *62* (9), 2177.
- (4) Bourgeois, O.; Skipetrov, S. E.; Ong, F.; Chaussy, J. *Phys. Rev. Lett.* **2005**, *94*, 057007.
- (5) Wang, X. X.; Getaneh, M.; Martoff, C. J.; Kaczanowicz, E. *J. Appl. Phys.* **1999**, *85*, 8274.
- (6) Roukes M. L.; et al. *Phys. Rev. Lett.* **1985**, *55*, 422–425.
- (7) Yung, C. S.; Schmidt, C. R.; Cleland, A. N. *Appl. Phys. Lett.* **2002**, *81*, 31.
- (8) Holmes, W.; Gildemeister, J. M.; Richards, P. L.; Kotsubo, V. *Appl. Phys. Lett.* **1998**, *72*, 2250.
- (9) Zeller, R. C.; Pohl, R. O. *Phys. Rev. B* **1971**, *4*, 2029.
- (10) Roukes, M. L. *Physica A* **1999**, *263*, 1.
- (11) Fon, W.; Schwab, K.; Worlock, J. M.; Roukes, M. L. *Phys. Rev. B* **2002**, *66*, 045302.
- (12) Tighe, T. S.; Worlock, J. M.; Roukes, M. L. *Appl. Phys. Lett.* **1997**, *70*, 2687.
- (13) Elgin, R. L.; Goodstein, D. L. *Phys. Rev. A* **1974**, *9*, 2657.
- (14) Schwab, K.; Henriksen, E. A.; Worlock, J. M.; Roukes, M. L. *Nature* **2000**, *404*, 976.
- (15) Schmidt, D. R.; Yung, C. S.; Cleland, A. N. *Appl. Phys. Lett.* **2003**, *83*, 1002–1004.

NL051345O